DNA-Tethered Hoechst Groove-Binding Agents: Duplex Stabilization and Fluorescence Characteristics

Kristin Wiederholt, Sharanabasava B. Rajur, John Giuliano, Jr., Maryanne J. O'Donnell, and Larry W. McLaughlin*

Contribution from the Department of Chemistry, Merkert Chemistry Center, Boston College, Chestnut Hill, Massachusetts 02167

Received March 22, 1996[⊗]

Abstract: Fluorescent Hoechst 33258 analogues have been synthesized in which the terminal phenol moiety is employed as a site for the introduction of a linker to permit covalent attachment of the fluorophores to oligo(deoxynucleotides). Hybridization by the DNA−Hoechst conjugates to target sequences generates the DNA minor groove structure and triggers a binding event by the tethered Hoechst agent. The attendant fluorescence signal reports upon this hybridization event. Conjugation of the Hoechst derivatives to the DNA sequences employs a cystamine linker tethered to an internucleotide phosphorus residue. This mode of conjugation maximizes the versatility of linker placement and minimizes the associated chemistry required to introduce the linker. Two related Hoechst derivatives have been synthesized; both contain a bromoacetamido linker for conjugation to the oligonucleotides. With each Hoechst derivative, two pairs of diastereomeric (R_p and S_p) oligo(deoxynucleotide) conjugates were prepared to provide the tethered Hoechst groove binders with two different orientations within the dA-dT rich minor groove. T_m measurements suggest that while all of the conjugates provide some increased duplex stability, the diastereomeric conjugates tentatively assigned the R_p configuration exhibit nearly 20 °C increases in T_m values for the double-stranded dodecameric complexes, while those tentatively assigned as the S_p diastereomers exhibit only moderate 4−8 °C increases in T_m values. The fluorescence characteristics of the conjugates are more variable, with one complex exhibiting a 23-fold enhancement in quantum yield effects, very similar to that observed for a free untethered Hoechst 33258 fluorophore bound to duplex DNA.

Introduction

A variety of extended heterocycles including Netropsin,[1] Distamycin,[2] DAPI,[3] and the Hoechst derivatives[4] bind tightly to duplex DNA.[5] On the basis of early chemical protection studies,[6] and more recent crystal structures,[1−4] binding by such agents occurs primarily in the minor groove of B-form duplexes at sequences containing from three to six dA-dT base pairs.[7] Binding appears to be mediated by the formation of specific hydrogen bonds to the O^2 oxygens of the dT residues and to the N^3 nitrogens of the dA residues in the target sites,[4] but electrostatic effects[8] or van der Waals contacts[9] may also be prominent between the binding agent and the "floor" or the "walls" of the minor groove. The extended heterocycles are capable of adopting a crescent shape that permits them to follow the convex curvature of the minor groove. They penetrate deeply into the minor groove and become "isohelical" with the B-form duplex.[10] Functional groups that protrude into the minor grove, such as the 2-amino group of dG-dC base pairs,[6a,11] or that of related base analogues such as 2-aminopurine,[12] interfere with optimal binding and give rise to the noted sequence preferences. Tight binding within the groove by such agents typically results in increased duplex stability.[13,14]

Ligands such as DAPI and the Hoechst derivatives are moderately fluorescent in aqueous solutions, but upon binding to double-stranded DNA exhibit a dramatically enhanced quantum yield,[15] some 20-fold greater than that observed for the free dyes.[16] The fluorescent properties of these agents have been employed to visualize chromosomes,[17,18] and to quantitate DNA concentrations.[19] The enhanced quantum yield effects are likely related to the tight binding by the ligand deep within the minor groove such that solvent access is restricted and non-radiative decay processes for the excited state are reduced.[15] A

* To whom correspondence should be addressed.

[⊗] Abstract published in *Advance ACS Abstracts,* July 15, 1996.

(1) (a) Kopka, M.; Yoon, C.; Goodsell, D.; Pjura, P.; Dickerson, R. E. *J. Mol. Biol.* **1985**, *183*, 55−61. (b) Kopka, M. L.; Yoon, C.; Goodsell, D.; Pjura, P.; Dickerson, R. E. *Proc. Natl. Acad. Sci. U.S.A.* **1985**, *82*, 1376−1380.

(2) Coll, M.; Frederick, C. A.; Wang, A. H.-J. *Proc. Natl. Acad. Sci. U.S.A.* **1987**, *84*, 8385−8389.

(3) Larsen, T. A.; Goodsell, D. S.; Cascia, D.; Grzeskowiak, K.; Dickerson, R. W. *J. Biomol. Stereodyn.* **1989**, *7*, 477−491.

(4) (a) Pjura, P. E.; Grzeskowiak, K.; Dickerson, R. E. *J. Mol. Biol.* **1987**, *197*, 257−271. (b) Teng, M.-K.; Usman, N.; Frederick, C. A.; Wang, A. H.-J. *Nucleic Acids Res.* **1988**, *16*, 2671−2675. (c) de C. T. Carrondo, M. A. A. F.; Coll, M.; Aymami, J.; Wang, A. H.-J.; van der Marel, G. A.; van Boom, J. H.; Rich, A. *Biochemistry* **1989**, *28*, 7849−7859.

(5) Dervan, P. B. *Science* **1986**, *232*, 464−471.

(6) (a) Harshman, K. D.; Dervan, P. B. *Nucleic Acids Res.* **1985**, *13*, 4825−4835. (b) Portugal, J.; Waring, M. J. *Biochim. Biophys. Acta* **1988**, *949*, 158−168. (c) Portugal, J.; Waring, M. J. *Eur. J. Biochem.* **1987**, *167*, 281−289. (d) Fox, K. R.; Waring, M. J. *Nucleic Acids Res.* **1984**, *12*, 9271−9285. (e) van Dyke, M. W.; Hertzberg, R. P.; Dervan, P. B. *Proc. Natl. Acad. Sci. U.S.A.* **1982**, *79*, 5470−5474.

(7) Abu-Daya, A.; Brown, P. M.; Fox, K. R. *Nucleic Acids Res.* **1995**, *23*, 3385−3392.

(8) Kissinger, K. L.; Drowicki, K.; Dabrowiak, J. C.; Lown, J. W. *Biochemistry* **1987**, *26*, 5590−5595.

(9) Lee, M.; Drowicki, K.; Hartley, J. A.; Pon, R. T.; Lown, J. W. *J. Am. Chem. Soc.* **1988**, *110*, 3641−3649.

(10) Goodsell, D.; Dickerson, R. E. *J. Med. Chem.* **1986**, *29*, 727−733.

(11) Martin, R. F.; Holmes, N. *Nature* **1983**, *302*, 452−454.

(12) Loontiens, F. G.; McLaughlin, L. W.; Diekmann, S.; Clegg, R. M. *Biochemistry* **1991**, *30*, 182−189.

(13) Jin, R.; Breslauer, K. J. *Proc. Natl. Acad. Sci. U.S.A.* **1988**, *85*, 8939−8942.

(14) Marky, L. A.; Breslauer, K. J. *Proc. Natl. Acad. Sci. U.S.A.* **1987**, *84*, 4359−4363.

(15) Zimmer, C.; Wähnert, U. *Prog. Biophys. Mol. Biol.* **1986**, *47*, 31−112.

(16) Lootiens, F. G.; Regenfuss, P.; Zechel, A.; Dumortier, L.; Clegg, R. M. *Biochemistry* **1990**, *29*, 9029−9039.

(17) Latt, S. A.; Wohlleb, J. C. *Chromosoma* **1975**, *52*, 297−316.

(18) Stokke, T.; Steen, H. B. *Cytometry* **1986**, *7*, 227−234.

(19) Kapuscinski, J.; Skoczylas, B. *Anal. Biochem.* **1977**, *83*, 252−257.

S0002-7863(96)00948-1 CCC: $12.00

variety of Hoechst analogues have been prepared to date.[20] In most of these studies, the interest in the analogues has been to alter base specificity by altering functional group interactions between the dye and the minor groove. In some cases, the modified Hoechst derivatives have been shown to bind to altered sequences, most notably to those containing a dG-dC base pair as part of a dA-dT binding site,[20a,g] or even to a dG-dC rich binding site.[21] Most of the analogues described in such studies still exhibit enhanced quantum yield effects upon binding to double-stranded DNA. Those studies suggest the possibility of functionalizing the Hoechst dye with a linker in order to provide a site for covalent attachment of the fluorophore to a DNA probe sequence without deleterious effects on the attendant fluorescent characteristics.

Covalent tethering of fluorophores and other agents to DNA has been accomplished by a number of protocols.[22] Virtually any functional group present in the DNA sequence, whether it is located on a base residue, carbohydrate, or internucleotide phosphorus, can be exploited for postsynthetic conjugation reactions.[23] Most commonly a short tether is introduced into the sequence to provide a terminal aliphatic amino or thiol group as the site for conjugation. Such tethers have been commonly employed at the 5′-terminus of the DNA sequence,[24] or internally using the C-5 position of dT,[25] one of the base amino groups,[26] the 2′-hydroxyl of a single ribonucleotide,[27] or one of the prochiral oxygens of an internucleotide phosphodiester.[28,29] A variety of agents have been tethered to DNA sequences to improve antisense or antigene activities by stabilizing duplex and triplex structures; such agents have included intercalators[30] and polypeptides[31] or peptide-like agents.[32]

Tethering an appropriate groove-binding fluorophore to a short DNA sequence should permit the development of a probe, which upon hybridization to a complementary target sequence generates the minor-groove-binding site and triggers a binding event by the tethered agent. Formation of a complex between the groove-binding agent and the hybridization product should result in enhanced thermal stability, and should generate a spectroscopic signal to report upon the occurrence of the hybridization event. A conjugate of this type could function as a valuable solution-based diagnostic or *in situ* hybridization probe. In this study we describe the synthesis of Hoechst-33258 derivatives appropriately modified with linkers that allow covalent attachment to DNA sequences. We report upon the covalent conjugation of such agents to DNA as well as the helix-stabilizing and fluorescent properties resulting from hybridization of these DNA−Hoechst conjugates to target sequences.

Experimental Section

Materials. Oligo(deoxynucleotides) were synthesized using 2′-deoxynucleoside phosphoramidites on an Applied Biosystems 381A DNA synthesizer. The four common 2′-deoxynucleoside phosphoramidites containing aryl- or isobutyrylamides were purchased from Cruachem through Fisher Chemical Co. H-phosphonate derivatives were obtained from Glen Research (Sterling, VA). The controlled pore glass support containing the 3′-terminal nucleoside was a product of CPG Inc. (Fairfield, NJ). Cystamine dihydrochloride, adamantanecarbonyl chloride, anhydrous solvents, and ammonium hydroxide were all obtained from the Aldrich Chemical Co. (Milwaukee, WI).

Nuclease P1 and snake venom phosphodiesterase were products of Boehringer Mannheim (Indianapolis, IN). Acrylamide and bisacrylamide were obtained from ICN Biomedicals (Cleveland, OH). Thin layer chromatography was performed on aluminum-backed precoated silica gel 60 F254 plates purchased from EM Science (Gibbstown, NJ). NMR spectra were obtained at 300 MHz on a Varian XL-300 multinuclear NMR spectrometer (residual solvent and water peaks present in the spectra have not been reported). UV measurements for thermal denaturation studies employed an AVIV 14DS spectrophotometer equipped with digital temperature control. Fluorescence emission spectra were collected on a Shimadzu RF5000U fluorescence spectrophotometer containing a Shimadzu DR-15 microprocessor and graphics display terminal. Mass spectra were obtained using FAB ionization from the Mass Spectrometry Laboratory, School of Chemical Sciences, University of Illinois, Urbana, IL.

Methods. 2-[2-(4-Nitrophenyl)-6-benzimidazolyl]-6-(1-methyl-4-piperazinyl)benzimidazole (3). To 0.35 g (1.08 mmol) of 2-(3,4-diaminophenyl)-6-(1-methyl-4-piperazinyl)benzimidazole (**1**)[33] dissolved in anhydrous methanol was added 0.46 g (2.17 mmol) of 4-nitrobenzimidic acid methyl ester (**2**)[34] followed by 0.13 mL (2.17 mmol) of glacial acetic acid. The mixture was refluxed for 2 h. At this point TLC analysis (dichloromethane/methanol, 1:1) indicated the complete absence of **1**. The solution was basified with ammonium hydroxide and the resulting precipitate collected. This material was purified by flash chromatography to yield 0.28 g (0.622 mmol) of **3** (57% yield). R_f (dichloromethane/methanol, 1:1): 0.56. ^{1}H-NMR (DMSO-d_6): $\delta = 2.00$ (s, 3H, NCH_3), 2.80 (s, 4H, $-CH_2-$), 3.20 (s, 4H, $-CH_2-$), 6.6−8.0 (m, 6H, Ar H), 8.20 (q, 4H, Ar H) ppm. UV (H_2O): $\lambda_{max} = 265$, 342 $\lambda_{min} = 304$ nm. IR (KBr): 3114, 2931, 2848, 2804, 1632, 1604, 1521, 1449, 1340, 1290, 1180, 1144, 857, 812, 708 cm^{-1}. Mass spectrum: calcd for $C_{25}H_{24}N_7O_2$ ($M + H^+$), 454.199 91, found 454.199 50.

2-[2-(4-Aminophenyl)-6-benzimidazolyl]-6-(1-methyl-4-piperazinyl)benzimidazole (4). To 0.27 g (0.60 mmol) of 2-[2-(4-nitrophenyl)-6-benzimidazolyl]-6-(1-methyl-4-piperazinyl)benzimidazole (**3**) in anhydrous methanol (15 mL) was added 0.13 g of Pd/C. The reaction mixture was stirred under a hydrogen atmosphere (1 atm) for 2 h. TLC analysis (dichloromethane/methanol, 1:1) after this time indicated the absence of starting material and the presence of a new product. The reaction mixture was filtered through Celite, and the resulting filtrate was evaporated to dryness. The product was purified by flash chromatography to yield 0.21 g (0.50 mmol) of **4** as a yellow solid

(20) (a) Latt, S. A.; Stetten, G. *J. Histochem. Cytochem.* **1976**, *24*, 24−33. (b) Bathini, Y.; Rao, K. E.; Shea, R. G.; Lown, J. W. *Chem. Res. Toxicol.* **1990**, *3*, 268−280. (c) Gupta, R.; Wang, H. Y.; Huang, L. R.; Lown, J. W. *Anti-Cancer Drug Des.* **1995**, *10*, 25−41. (d) Gravatt, G. L.; Baguley, B. C.; Wilson, W. R.; Denny, W. A. *J. Med. Chem.* **1994**, *37*, 4338−4345. (e) Czarny, A.; Boykin, D. W.; Wood, A. A.; Nunn, C. M.; Neidle, S.; Zhao, M.; Wilson, W. D. *J. Am. Chem. Soc.* **1995**, *117*, 4716−4717. (f) Beerman, T. A.; McHugh, M. M.; Sigmund, R.; Lown, J. W.; Rao, K. E.; Bathini, Y. *Biochim. Biophys. Acta* **1992**, *1131*, 53−61. (g) Parkinson, J.; Sadat-Ebrahimi, S.; Wilton, A.; McKie, J. H.; Andrews, J.; Douglas, K. T. *Biochemistry* **1995**, *34*, 16240−16244.

(21) Singh, M. P.; Joseph, T.; Kumar, S.; Bathini, Y.; Lown, J. W. *Chem. Res. Toxicol.* **1992**, *5*, 597−607.

(22) Goodchild, J. *Bioconjugate Chem.* **1990**, *1*, 165−187.

(23) O'Donnell, M.; McLaughlin, L. W. In *Bioorganic Chemistry: Nucleic Acids*; Hecht, S., Ed.; Oxford University Press: Oxford, 1996; pp 216−243.

(24) (a) Agrawal, S.; Christodoulou, C.; Gait, M. J. *Nucleic Acids Res.* **1986**, *14*, 6227−6245. (b) Connolly, B. A. *Nucleic Acids Res.* **1987**, *15*, 3131−3139 (c) Coull, J. M.; Weith, H. L.; Bischoff, R. *Tetrahedron Lett.* **1986**, *27*, 3991−3994.

(25) Bergstrom, D. E.; Ruth, J. L. *J. Am. Chem. Soc.* **1976**, *98*, 1587−1589.

(26) MacMillan, A. M.; Verdine, G. L. *J. Org. Chem.* **1991**, *55*, 5931−5933.

(27) Manoharan, M.; Guinosso, C. J.; Cook, P. D. *Tetrahedron Lett.* **1991**, *32*, 7171−7174.

(28) (a) Fidanza, J. A.; McLaughlin, L. W. *J. Am. Chem. Soc.* **1989**, *111*, 9117−9120. (b) Fidanza, J.; McLaughlin, L. W. *J. Org. Chem.* **1992**, *57*, 2340−2346. (c) Fidanza, J. A.; Ozaki, H.; McLaughlin, L. W. *J. Am. Chem. Soc.* **1992**, *114*, 5509−5517.

(29) Jäger, A.; Levy, M. H.; Hecht, S. M. *Biochemistry* **1988**, *27*, 7237−7246.

(30) Thuong, N. T.; Asseline, U.; Moneney-Garestier, T. In *Oligodeoxynucleotides. Antisense Inhibitors of Gene Expression*; Cohen, J., Ed.; CRC Press, Inc.: Boca Raton, FL, 1989; pp 25−48.

(31) Lemaitre, M.; Bayard, B.; Lebleu, B. *Proc. Natl. Acad. Sci. U.S.A.* **1987**, *84*, 648−652.

(32) Sinyakov, A. N.; Lokhov, S. G.; Kutyavin, I. V.; Gamper, H. B.; Meyer, R. B. *J. Am. Chem. Soc.* **1995**, *117*, 4995−4996.

(33) Loewe, H.; Urbanietz, J. *Arzneim.-Forsch.* **1974**, *27*, 1927−1933.

(34) Prepared by dissolving 4-nitrobenzonitrile in methanol and bubbling anhydrous HCl through the solution. The precipitate formed (**5**) was collected, dried, and used without further purification.

(83% yield). R_f (dichloromethane/methanol, 7:3, + trace of tri-*n*-butylamine): 0.36. ^{1}H-NMR (DMSO-d_6): δ = 2.10 (s, 3H, NCH_3), 3.00 (s, 4H, $-CH_2-$), 3.10 (s, 4H, $-CH_2-$), 5.60 (s, 2H, $-NH_2$), 6.4−8.2 (m, 10 H, Ar H). UV (H_2O): λ_{max} 272, 342, λ_{min} 254, 298 nm. IR (KBr): 2933, 2808, 1608, 1439, 1491, 1280, 1234, 1178, 1140, 1005, 963, 832 cm^{-1}. HRMS: calcd for $C_{25}H_{26}N_7$ (M + H$^+$), 424.224 97, found 424.224 50.

2-[2-[4-(Bromoacetamido)phenyl]-6-benzimidazolyl]-6-(1-methyl-4-piperazinyl)benzimidazole (5). To 0.1 g (0.236 mmol) of 2-[2-(4-aminophenyl)-6-benzimidazolyl]-6-(1-methyl-4-piperazinyl)benzimidazole (**4**) dissolved in a mixture of DMF/dichloromethane (1:1, v/v) (4 mL) cooled to −78 °C was added 0.26 mL (0.472 mmol) of bromoacetic anhydride followed by 0.028 g (0.023 mmol) of 4-(*N*,*N*-dimethylamino)pyridine. The reaction mixture was stirred at −78 °C for 3 h. TLC analysis (dichloromethane/methanol, 7:3, + trace tri-*n*-butylamine) indicated the completion of the reaction. Methanol (1 mL) and then water (1 mL) were added at −78 °C to destroy any unreacted bromoacetic anhydride. The solvents were evaporated, and the residue was dissolved in the minimum amount of methanol and added to ether. The resulting yellow precipitate was filtered and washed thoroughly with ether. The resulting yellow solid was purified on a small column of silica gel using a gradient of dichloromethane and methanol. The pooled fractions were evaporated to yield 0.098 g (0.234 mmol) of **5** (97% yield). R_f (dichloromethane/methanol, 7:3, + trace of tri-*n*-butylamine): 0.52. ^{1}H-NMR (DMSO-d_6): δ = 2.25 (s, 3 H, NCH_3), 2.50 (m, 8 H, $-CH_2-$), 4.25 (s, 2 H, bromoacetyl H), 6.95 (d, 1 H, Ar H), 7.05 (s, 1 H, Ar H), 7.45 (d, 1 H, Ar H), 7.71 (d, 1 H, Ar H), 7.82 (d, 2 H, Ar H), 8.04 (d, 1 H, Ar H), 8.19 (d, 2 H, Ar H), 8.38 (s, 1 H, Ar H), 10.43 (s, 1 H, amido H) ppm. The imidazole NH residues could not be located under these solvent conditions. The amide resonance at 10.43 ppm was exchangeable. UV (H_2O): λ_{max} 268, 345 nm, λ_{min} 245, 296 nm. HRMS: calcd for $C_{27}H_{27}N_7BrO$ (M + H$^+$), 544.146 04, found 544.144 00.

2-[2-[4-[2-(Trifluoroacetamido)ethoxy]phenyl]-6-benzimidazolyl]-6-(1-methyl-4-piperazinyl)benzimidazole (7). 4-[2-(Trifluoroacetamido)ethoxy]benzonitrile was prepared by the condensation of (*tert*-butoxycarbonyl)ethanolamine with 4-cyanophenol using a Mitsonobu protocol.[35] The *tert*-butoxycarbonyl group was removed by passing HCl(g) through the crude product dissolved in dichloromethane, and the resulting amine was protected with trifluoroacetic anhydride in quantitative yield using a standard literature procedure.[36]

To prepare the necessary imino methyl ester **6**, 1.2 g (4.65 mmol) of 4-[2-(trifluoroacetamido)ethoxy]benzonitrile was dissolved in 15 mL of dichloromethane, 0.267 g (8.37 mmol) of anhydrous methanol was added, and the reaction was cooled to 0 °C. The reaction mixture was saturated with HCl(g) and maintained at 0 °C overnight. The resulting white precipitate was collected, washed thoroughly with diethyl ether, and dried to yield 1.3 g (4.40 mmol, 96%) of a white solid which was used in the following step without purification.

To 100 mg (0.310 mmol) of 2-(3,4-diaminophenyl)-6-(1-methyl-4-piperazinyl)benzimidazole (**1**)[33] dissolved in 3 mL of anhydrous methanol was added 134 mg (0.465 mmol) of 4-[2-(trifluoroacetamido)-ethoxy]benzimidic acid methyl ester followed by 37 μL (∼0.6 mmol) of glacial acetic acid. The mixture was stirred at 65−70 °C for 3 h. At this time, TLC analysis (dichloromethane/methanol, 7:3, containing a trace of tri-*n*-butylamine) indicated the absence of starting material and the presence of a new compound that was fluorescent under long-wavelength UV excitation (365 nm). Solvents were removed by evaporation, the residue was dissolved in a minimum amount of methanol, and the solution was neutralized with ammonium hydroxide. The resulting brown precipitate was collected and purified by silica gel column chromatography (dichloromethane and a gradient of methanol, containing a trace amount of tri-*n*-butylamine) to yield 80 mg (0.138 mmol, 45%) of **7**. R_f (dichloromethane/methanol, 7:3, containing a trace of tri-*n*-butylamine): 0.38. ^{1}H-NMR (DMSO-d_6): δ = 2.2 (s, 3H, CH_3), 3.0−3.2 (m, 8H, $-CH_2-$), , 3.6 (t, 2H, $-CH_2-$), 4.2 (t, 2H, $-CH_2-$), 6.9 (d, 2H, Ar H), 7.1 (d, 2H, Ar H), 7.4 (s, 1H, Ar H), 7.6 (s, 1H, Ar H), 7.9 (d, 1H, Ar H), 8.2 (d, 2H, Ar H) 8.3 (s, 1H, Ar H), 9.8 (s, 1H, NH) ppm. UV (methanol): λ_{max} 254, 330 nm, λ_{min} 296 nm. HRMS: calcd for $C_{29}H_{29}N_7O_2F_3$ (M + H$^+$), 564.233 48, found 564.232 30.

2-[4-(2-Aminoethoxy)phenyl]-6-benzimidazolyl]-6-(1-methyl-4-piperazinyl)benzimidazole (8). The trifluoroacetamide **7** (140 mg, 0.248 mmol) was dissolved in 10 mL of potassium carbonate in methanol and water (5:2, v/v). The turbid solution was heated gently until a clear solution resulted and then allowed to stir overnight at ambient temperature. TLC analysis at this point indicated that the starting material was absent and a new fluorescent spot was present. The solvents were removed, and the residue **8** was purified by flash chromatography on silica gel (dichloromethane with a gradient of methanol containing trace amounts of tri-*n*-butylamine to yield 110 mg of **8** (0.235 mmol) 94%. R_f (dichloromethane/methanol, 1:1, containing a trace of tri-*n*-butylamine): 0.18. ^{1}H-NMR (DMSO-d_6): δ = 2.2 (s, 3H, $-CH_3$), 2.4−2.8 (m, 8H, $-CH_2-$), 3.0 (t, 2H, $-CH_2-$), 4.0 (t, 2H, $-CH_2-$), 5.4 (s, 2H, $-NH_2$), 6.9 (d, 2H, Ar H), 7.1 (d, 2H, Ar H), 7.4 (d, 1H, Ar H), 7.6 (d, 2H, Ar H), 7.9 (d, 1H, Ar H), 8.2 (d, 2H, Ar H), 8.24 (s, 1H, Ar H) ppm. UV (methanol): λ_{max} 254, 330 nm, λ_{min} 296 nm. HRMS: calcd for $C_{27}H_{30}N_7O$ (M + H$^+$), 468.251 18, found 468.251 30.

2-[2-[4-[2-(Bromoacetamido)ethoxy]phenyl]-6-benzimidazolyl]-6-(1-methyl-4-piperazinyl)benzimidazole (9). To 50 mg (0.107 mmol) of **8** dissolved in 3 mL of anhydrous DMF was added ∼1 mg of 4-(*N*,*N*-dimethylamino)pyridine, and the solution was cooled to −78 °C. To the cooled solution was added 56 mg (0.214 mmol) of bromoacetic anhydride, and the reaction mixture was stirred for 3 h at −78 °C. TLC analysis after 3 h indicated the absence of starting material and the presence of a new compound. The reaction was quenched with methanol, and the mixture was reduced in volume. Ether was added, and the resulting precipitate was collected and purified by column chromatography on silica gel using a gradient of dichloromethane/methanol containing a trace amount of tri-*n*-butylamine to yield 35 mg (0.059 mmol, 56%) of **9**. R_f (dichloromethane/methanol, 7:3, containing a trace of tri-*n*-butylamine): 0.52. ^{1}H-NMR (DMSO-d_6): δ = 2.2 (s, 3H, $-CH_3$), 3.2−3.6 (m, 8H, $-CH_2-$), 3.8 (t, 2H, $-CH_2-$), 4.2 (t, 2H, $-CH_2-$), 4.4 (s, 2H, $-CH_2-$), 7.0−8.4 (m, 10H, Ar H), 9.0 (s, 1H, NH) ppm. UV (methanol): λ_{max} 255, 335 nm, λ_{min} 295 nm. HRMS: calcd for $C_{29}H_{31}N_7O_2Br$ (M + H$^+$), 588.172 26, found 588.171 40.

Synthesis of Oligonucleotides Tethering a Masked Thiol Group (10). DNA sequences were initially assembled using phosphoramidite protocols.[37] At the site of the tether, 25 μmol of the appropriate fully protected nucleoside H-phosphonate was dissolved in 600 μL of 1:1 anhydrous acetonitrile/pyridine and activated by the addition of 25 μmol of adamantanecarbonyl chloride.[38,39] The column was removed from the synthesizer and the activated monomer was added using a syringe. The column was then rinsed with 1:1 anhydrous pyridine/acetonitrile, followed by acetonitrile, and was then dried in a desiccator under high vacuum. The *N*-(triphenylacetyl)cystamine linker was then added as described.[40] The remaining monomers were added using standard phosphoramidite protocols, but the capping steps were deleted.[40] After removal of the terminal DMT group, the sequences were deprotected (concentrated ammonia for 6 h at 50 °C), and the diastereomeric sequences were separated and isolated using a 9.4 × 250 mm column of ODS-Hypersil at a flow rate of 3.0 mL/min in 20 mM potassium phosphate (pH 5.5) with a gradient of methanol (0−100% over 90 min), desalted (Sephadex G-10), and lyophylized to dryness.

Oligonucleotide Conjugation. To 1 A_{260} unit of a single diastereomer of the desired dodecamer in 100 mM Tris·HCl, pH 8, was added DTT to a concentration of 10 mM, and the mixture was incubated at 50 °C for 1 h. HPLC analysis [50 mM triethylammonium acetate, pH 7.0, with a linear gradient of acetonitrile (7−28% over 30 min)] after this time period indicated the complete absence of the (triphenylmethyl)-acetyl-protected sequence (retention time ∼28 min) and the presence

(35) Mitsunobu, O. *Synthesis* **1981**, 1−28.
(36) Pyne, S. G. *Tetrahedron Lett.* **1987**, *28*, 4737−4741.
(37) Matteucci, M. D.; Caruthers, M. H. *J. Am. Chem. Soc.* **1981**, *103*, 3185−3191.
(38) Froehler, B. C.; Ng, P. G.; Matteucci, M. D. *Nucleic Acids Res.* **1986**, *14*, 5399−5407.
(39) Froehler, B. C.; Matteucci, M. D. *Tetrahedron Lett.* **1986**, *27*, 469−472.
(40) O'Donnell, M. J.; Hebert, N.; McLaughlin, L. W. *Biol. Med. Chem. Lett.* **1994**, *4*, 1001−1004.

of a new peak (retention time ~9 min). The bromoacetylated Hoechst derivative (**5** or **9**) in DMF was added to this reaction mixture to a concentration of 15 mM (40% DMF). The reaction mixture was shaken at ambient temperature for 48 h (a precipitate appeared during this period). An equal amount of formamide was added to the reaction mixtures, and they were heated to 90 °C (to dissolve aggregates) and loaded directly onto the gel for isolation by electrophoresis.

The conjugated product was purified on a 20% denaturing (7 M urea) polyacrylamide gel. A fluorescent band (365 nm excitation) was present whose position was retarded slightly with respect to the oligomer containing the free thiol linker. This band was excised from the gel, crushed, and soaked in 0.3 M sodium acetate, pH 6. The gel was removed and the product desalted using a C18 Sep-pak column and a water/methanol gradient. The conjugated oligomer was eluted with approximately 80% methanol in water. Yields varied, typically 0.3−0.5 A_{260} unit. The product exhibited a UV/vis spectrum having characteristics of both DNA (λ_{max} = 260 nm) and the Hoechst fluorophore (λ_{max} = 342 nm).

Nucleoside Analysis. Nucleoside composition was determined after nuclease P1/snake venom phosphodiesterase/bacterial alkaline phosphatase hydrolysis: A 20 μL reaction mixture containing 0.5 A_{260} unit of oligomer in 25 mM sodium acetate, pH 5.3, was incubated for 1 h at 37 °C with nuclease P1. The reaction mixture was then rebuffered to pH 8 with a solution of 100 mM Tris·HCl, pH 8.0; 10 mM $MgCl_2$, 3 units of snake venom phosphodiesterase, and 2 units of alkaline phosphatase were added, and the mixture was incubated for an additional 2 h at 37 °C. An aliquot containing approximately 0.2 A_{260} unit of material was analyzed by HPLC using a 4.6 × 250 mm column of ODS-Hypersil in 20 mM potassium phosphate, pH 5.5, and a gradient of 0−70% methanol (60 min) followed by isocratic elution with solvent B. The following retention times were observed (260 nm): (dC) 6.4, (dG) 10.4, (dT) 11.1, (dA) 14.2, (d[Tp($NHCH_2CH_2SH$)T]) 29.8 and 30.5, (d[Tp($NHCH_2CH_2$S-Hoechst)T]) 62 and 63.5 min (both Hoechst conjugates exhibited similar retention times).

***T*$_m$ Values.** T_m values were obtained for complexes containing a 1:1 mixture of the conjugate and its complementary sequence in 21 mM HEPES, pH 7.5, containing 100 mM NaCl and 20 mM $MgCl_2$ at duplex concentrations in the low micromolar range. Solutions were heated in 0.5 or 1.0 °C steps, and absorbance readings were taken after a period of temperature stabilization. Absorbance and temperature readings were plotted using Igor software. T_m values were determined from first- and second-order derivatives, as well as graphically from the absorbance vs temperature plots.

Fluorescence Measurements. Fluorescence measurements were made in solutions typically containing ~1 μM DNA−Hoechst conjugate in 21 mM HEPES, pH 7.5, containing 100 mM NaCl and 20 mM $MgCl_2$. All emission measurements were made with the following list of parameters: slit width Ex/Em = 5 nm/5 nm, high sensitivity, fast speed. Samples were introduced into a 1.25 mL cell thermally isolated with a water jacket. Temperature was controlled with a recirculating water bath. Fluorescence emissions were measured at 450 nm with an excitation wavelength of 342 nm. The ΔF values were ratios obtained at 450 nm. This emission wavelength represented the emission maximum for the duplex conjugates and was slightly off the emission maximum for the single-stranded conjugates.

Results

We have prepared oligonucleotides tethering the fluorescent minor-groove-binding agent Hoechst 33258. This dye exhibits both favorable helix-stabilizing properties[41] and enhanced fluorescence characteristics[12,16] upon binding to double-stranded DNA sequences. Both Hoechst 33258 and the related Hoechst 33342 derivative (differing only in the nature of the terminal phenol moiety) are similarly fluorescent. A variety of structurally related derivatives in which the terminal phenol moiety has been replaced with other functionality retain both the DNA-binding characteristics and the desired fluorescence properties.[20] Those observations suggested that the terminal phenol ring could

Scheme 1[a]

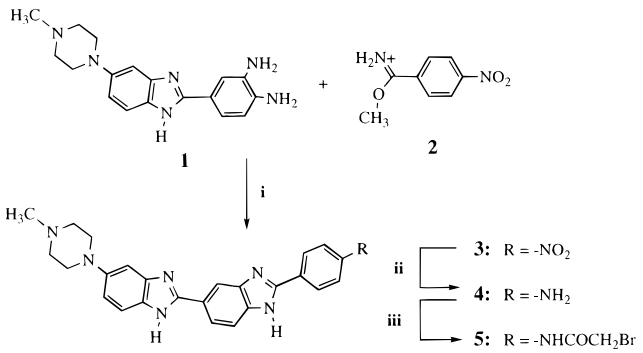

[a] Conditions: (i) CH_3COOH, heating. (ii) H_2/Pd−C. (iii) $(BrCH_2CO)_2$/DMAP, −78 °C.

be employed as a site for attachment of the desired linker without interfering with the fluorescent characteristics. Attempts to directly functionalize the phenolic hydroxyl of the native Hoechst 33258 fluorophore were unsuccessful. For this reason we chose to synthesize the bisbenzimidazole ring system in order to vary the functionality of the fluorophore as needed.

Synthesis of the Hoechst Fluorophores. The terminal phenol residue is introduced relatively late in the described synthetic procedure.[33] We simply altered the final portions of the known synthetic pathway as needed to modify the character of this terminal phenol. For example, after preparation of 2-(3,4-diaminophenyl)-6-(1-methyl-4-piperazinyl)benzimidazole (**1**; Scheme 1),[33] we introduced a terminal anilino residue to provide a site to tether a bromoacetamido linker (see **5**; Scheme 1). The synthesis of **5** proceeded without difficulty; we simply altered the final cyclization step by incorporating a nitrophenyl moiety in place of the more common phenol to generate **3** (Scheme 1). The nitro group was subsequently reduced to the corresponding amino group which could then be acylated with bromoacetic anhydride to generate the Hoechst derivative **5**.

The related Hoechst derivative **9** extends the bromoacetamide linker away from the chromophore by inserting an additional two carbons between the phenylbisbenzimidazole chromophore and the bromoacetamido moiety. This derivative increases the length of the linker between the fluorophore and its site of attachment to the DNA. The two-carbon linker may also insulate the fluorescent bisbenzimidazole from any undesirable electronic effects resulting from the presence of the bromoacetamido group attached to the terminal aromatic ring of the chromophore. Compound **9** was prepared by a procedure similar to that described for **5**, and the route is outlined in Scheme 2. It involves the condensation of **1** with the imino methyl ester **6**. After removal of the trifluoroacetamide, the aminoethoxy derivative **8** was bromacetylated to generate **9**.

Synthesis of the DNA−Hoechst Conjugates. With both Hoechst derivatives **5** and **9** we have employed a terminal bromoacetamido moiety to permit covalent attachment to the DNA sequence. The bromoacetamido group has functioned well in previous studies as a thiol-specific alkylating agent for postsynthetic conjugation by a variety of fluorophores, or other agents, to thiol linkers present in DNA sequences.[28]

From the wide variety of techniques available to covalently attach reporter groups to DNA sequences,[22,28,29,40,42] we chose a backbone-labeling procedure[40,42] in which the reporter group is tethered to an internucleotide phosphorus residue. The

(41) Wilson, W. D.; Ratmeyer, L.; Zhao, M.; Strekowski, L.; Boykin, D. *Biochemistry* **1993**, *32*, 4098−4104.

(42) (a) Letsinger, R. L.; Schott, M. E. *J. Am. Chem. Soc.* **1981**, *103*, 7394−7398. (b) Yamana, K.; Letsinger, R. L. *Nucleic Acids Symp. Ser.* **1985**, *16*, 169−173. (c) Letsinger, R. L.; Bach, S. A.; Eadie, J. S. *Nucleic Acids Res.* **1986**, *14*, 3487−3497. (d) Agrawal, S.; Tang, J.-Y. *Tetrahedron Lett.* **1990**, *31*, 1543−1546.

Scheme 2[a]

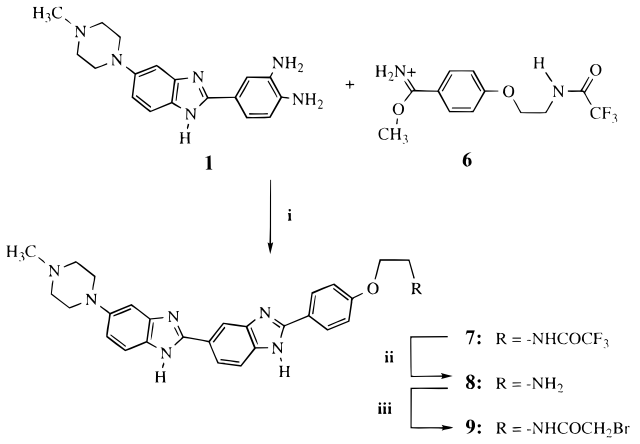

[a] Conditions: (i) CH_3COOH, heating. (ii) K_2CO_3/CH_3OH. (iii) $(BrCH_2CO)_2$/DMAP, −78 °C.

Scheme 3[a]

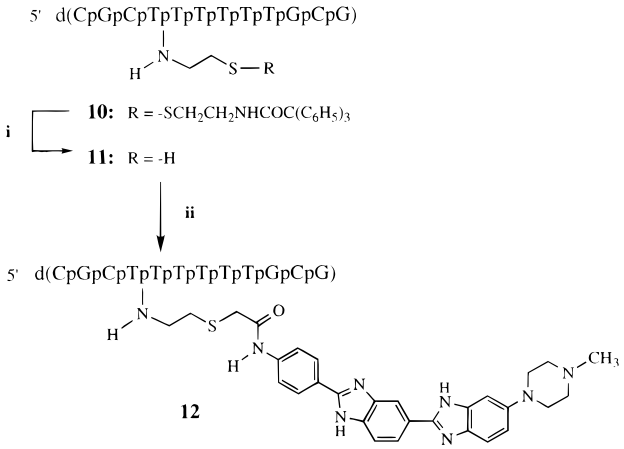

[a] Conditions: (i) DTT. (ii) **5**, 48 h, ambient temperature, PAGE.

reasons for this choice were fourfold: (i) Locating the tether on the internucleotide phosphorus places the groove-binding agent on the outer surface of the nucleic acid duplex structure where it is unlikely to interfere with base−base hydrogen-bonding interactions between the probe and the target sequence. (ii) By using the internucleotide phosphorus as the site of attachment, the tether can be easily moved from one internucleotide linkage to another to explore variations in the positioning of the tethered groove-binding agent within a given sequence. (iii) Tethering the reporter group to an internucleotide phosphorus residue places it in two diastereomeric positions about the internucleotide phosphorus; one diastereomer may be more effective in directing the Hoechst derivative toward the minor-groove binding site. (iv) In principle, the groove-binding agent could have been simply attached to one terminus of the probe sequence, but positioning the groove-binding agent near the end of a dA-dT rich duplex might be deleterious in that only a portion of the groove-binding agent would be able to effectively interact within the groove structure due to potential end-fraying effects. More efficient groove binding might result if such derivatives were attached to the DNA backbone near the center of the short duplex sequence, at the point where the duplex exists as a well-formed structure.

The DNA containing the thiol tether was synthesized using standard phosphoramidite-based procedures until the site for attachment of the tether was reached. At this point, a nucleoside residue containing an H-phosphonate internucleotide linkage[43] was incorporated into the growing oligonucleotide chain and immediately oxidized in the presence of carbon tetrachloride/pyridine and *N*-(triphenylacetyl)cystamine.[40] This procedure results in the incorporation of a phosphoramidate internucleotide linkage at the site of choice, tethering a masked thiol. Owing to the presence of two prochiral nonbridging oxygens, the phosphoramidate is formed as a diastereomeric pair. The bulky triphenylacetyl residue attached to the tether (see **10**; Scheme 3) results in differential chromatographic mobilities sufficient to permit effective resolution of the two isomeric phosphoramidates. To date we have not been able to unambiguously assign the absolute configurations of the two phosphoramidate stereocenters, and have simply labeled them according to their relative elution order from a reversed phase column using HPLC analyses. For example, **10a** elutes from the HPLC column "earlier" than **10b**.

Synthesis and isolation of a single isomer of a dodecamer containing a masked thiol tether, for example (see **10**; Scheme 3), was followed by reduction of the unsymmetrical disulfide with tris(2-carboxyethyl)phosphine[44] or DTT to eliminate the triphenylacetyl moiety and unmask the thiol labeling site (**11**). For each diastereomer, the free thiol of **10** (or corresponding dA sequence) was reacted with an excess of **5** or **9** in an aqueous/DMF (60:40) solution at pH 8.0. The conjugation reaction functioned best with concentrations of DNA and reporter group in the low millimolar range, but the reaction was complicated by the fact that Hoechst 33258 is known to aggregate in aqueous solutions at concentrations near or above 30 μM.[16] The use of high concentrations of *N*,*N*-dimethylformamide reduced such aggregation and maximized the solubility of the fluorophore without precipitating the thiol-containing DNA. To compensate for aggregation problems present during isolation of the DNA conjugate, it was necessary to resolve the product from the heterogeneous reaction mixture by employing a denaturing (7 M urea) polyacrylamide gel. Each conjugate could be excised from the gel, extracted, and desalted to generate a purified DNA−Hoechst conjugate (e.g., **12** in Scheme 3). The purified conjugates were solubilized in aqueous solution at concentrations of not more than ∼10 μM, and analyzed by reversed phase HPLC. Such analyses resulted in the elution of a single peak (see the supporting information). The isolated materials exhibited absorption characteristics for both the DNA ($\lambda_{max} = 260$ nm) and the Hoechst groove binder ($\lambda_{max} = 342$ nm). Digestion of the conjugates by a mixture of nucleases and alkaline phosphatase, followed by HPLC analysis, resulted in a chromatogram indicating the presence of the common nucleosides, and a strongly retained species corresponding to the material obtained when one isomer of the dimer d[Tp($NHCH_2CH_2SH$)T] was conjugated to **5** or **9**. Using this approach, both phosphorus diastereomeric conjugates of **12** (Scheme 3) were prepared, as were both diastereomers of the corresponding dA rich sequence d[CpGpCAp($NHCH_2CH_2S$-Hoechst)ApApApApApGpCpG] (**13**). Each of the diastereomeric pairs are differentiated only by their relative elution time from the HPLC column. For example, **12a** represents the early eluting diastereomer for the conjugate prepared from **10a**, while **12b** represents the later eluting isomer prepared from **10b**. Each pair of diastereomeric conjugates, upon complexing to the complementary target sequence, is provided with a 5−6 base pair binding site composed of dA-dT base pairs. Attachment of the groove binding agent to either the dT-containing (**12a**/**12b**) or the dA-containing (**13a**/**13b**) sequence has the effect of placing the covalent tether in one of the two possible

(43) Froehler, B. C. *Tetrahedron Lett.* **1986**, *27*, 5575−5578.

(44) Burns, J. A.; Butler, J. C.; Moran, J.; Whitesides, G. M. *J. Org. Chem.* **1991**, *56*, 2648−2650.

Table 1. Helix Stabilization and Fluorescence Characteristics of DNA−Hoechst Conjugates

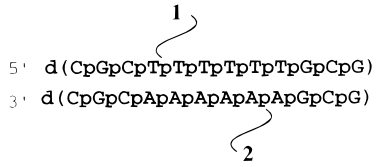

conjugate	Hoechst derivative	site of conjugation	isomer[a]	T_m[b] (°C)	ΔF[c]
native duplex				55 ± 1	nf[d]
10		1	**a**	51	nf
10		1	**b**	51	nf
12	**5**	1	**a**	74	6
12	**5**	1	**b**	59	6
13	**5**	2	**a**	74	7
13	**5**	2	**b**	63	4
14	**9**	1	**a**	73	23
14	**9**	1	**b**	61	12
15	**9**	2	**a**	74	12
15	**9**	2	**b**	61	11

[a] Isomer designations "**a**" and "**b**" were assigned according to the relative elution order of the phosphorus diastereomers of **10** (or the corresponding dA-containing sequence) during HPLC isolation procedures. In each case, the corresponding Hoechst conjugation isomer results from the reaction of the same isomer of **10** (or the corresponding dA-containing sequence). For example, **12a** was generated from **10a**, while **12b** resulted from **10b**). [b] Values are reported in °C for the conjugate shown complexed to its native complementary sequence, 5′-d(CpGpCpApApApApApApGpCpG) or 5′-d(CpGpCpTpTpTpTpTpTpGpCpG), and were obtained in 21 mM HEPES, pH 7.0, containing 100 mM NaCl and 20 mM $MgCl_2$. Each value is the average of two or more determinations, and the precision is estimated to be ±1 °C. [c] Values represent the fluorescence enhancement ratio observed at 450 nm upon adding 1 equiv of the complementary native sequence. [d] nf = no fluorescence.

diastereomeric positions, as well as at two different positions on the DNA (at opposite ends of the minor-groove-binding site).

In similar fashion, we prepared the diastereomeric conjugates **14** and **15,** again beginning with **10** (or the dA-containing sequence) but using the Hoechst derivative **9** containing the two-carbon spacer separating the terminal phenyl ring from the reactive bromoacetamido linker. The isolation, analysis, and identification of the diastereomeric pairs **14a**/**14b** and **15a**/**15b** proceeded in a manner strictly analogous to that described above for **12** and **13**.

Helix-Stabilizing Properties. Absorbance vs temperature plots for the native dodecameric duplex (see Table 1) (∼1 μM) in the presence of free Hoechst 33258, or either of the analogues **5** and **9**, at a concentration of 1.2, 5, or 10 μM, all resulted in very similar T_m values varying from 62 to 65 °C. These T_m values, measured in the presence of the various free fluorophores, were 7−10 °C higher than the T_m value observed for the native duplex (T_m = 55 °C).

The helix-stabilizing properties of the conjugated sequences were evaluated by adding between 1.0 and 1.2 equiv of the native complementary sequence and then analyzing the variation in T_m values under a common set of buffer and salt conditions. Conjugating a large bulky group to a DNA duplex, in the absence of any specific binding effects, can result in helix destabilization as noted for **10a**/**10b** (Table 1). Complexes containing one of the conjugated dodecameric sequences all exhibited increased T_m values (Table 1). The DNA duplex formed from **12a** and its complement exhibited a 19 °C increase in T_m relative to that of the unmodified duplex. By comparison, the duplex containing the corresponding diastereomer **12b** resulted in a more moderate increase of 4 °C. Relative to the diastereomeric complexes of **12**, the DNA duplexes formed from **13a** and **13b** result in the Hoechst derivative being tethered at the opposite end of the minor-groove-binding site. This variation in location should have the effect of reversing the orientation of the groove-binding fluorophore within the minor groove. The T_m values measured for complexes containing **13a** and **13b** were 74 and 63 °C, respectively, similar in both cases to the values observed for the corresponding diastereomers of **12** (Table 1). With both conjugates **12** and **13**, one diastereomer (isomer **a**) resulted in a higher T_m value for the duplex.

Conjugates **14** and **15** were prepared from **9**, which contains a linker lengthened by two additional carbon atoms. This increase in length should provide more flexibility for the Hoechst fluorophore. As noted for the conjugates **12** and **13**, conjugates **14** and **15** are designed as positional isomers, with the Hoechst derivative being tethered at either end of a stretch of dA-dT base pairs. Similar to the results noted for **12** and **13**, both DNA duplexes containing diastereomers **14a** and **15a** exhibited T_m values increased by 18−19 °C relative to that of the native duplex. By comparison, **14b** and **15b** exhibited more moderate increases of 6 °C. A diastereomeric mixture of **14a**/**14b** (40:60) resulted in a T_m increase of intermediate value (∼13 °C).

In contrast to the variation in T_m values observed for diastereomeric pairs of conjugates, the position of the conjugated dye, with respect to its orientation in the minor groove, had little impact upon the T_m values for the conjugated duplexes. The two conjugate pairs **12a** and **13a** and then **14a** and **15a** position the Hoechst derivatives in opposite relative orientations within the DNA minor groove [the same relationship is present for the pair **12b** and **13b** (or **14b** and **15b**)]. However, regardless of such orientation effects, the T_m values remained largely unchanged for various positional isomers. Both **12a** and **13a** exhibited the same 19 °C increase in T_m values, and corresponding similarities were observed for **14a** and **15a**. In a similar manner, **12b** and **13b** (as well and **14b** and **15b**) all exhibited T_m values largely independent of the position of the Hoechst derivative.

Fluorescence Characteristics. We initiated our fluorescence studies by examining the characteristics of a 1 μM solution of Hoechst 33258 titrated with the native dodecameric duplex 5′-d(CpGpCApApApApApApGpCpG)•d(CpGpCpTpTpTpTpTpTpGpCpG). The 1:1 complex of DNA and dye exhibited (λ_{ex} = 342 nm, λ_{em} = 450 nm) an enhancement in emission maximum (ΔF) of 26, a value that is consistent with previous studies[16] employing the dodecamer [d(CpGpCpGpApApTpTpCpGpCpG)]$_2$. In this related work a value for ΔF of approximately 30 was reported. In similar experiments we observed ΔF values of 11 and 19, for 1:1 complexes of the native duplex dodecamer and the Hoechst derivative **5** or **9**, respectively. We recognized that at concentrations in the low micromolar range the possibility existed for multiple modes of binding by these bisbenzimidazoles,[16] not all of which would necessarily result in significant enhancement of fluorescence properties, but as an important control experiment, we needed to quantify the fluorescence characteristics for the untethered fluorophores bound to the target duplex under conditions where T_m values and fluorescence properties of the conjugated complexes would be studied.

Each conjugate **12**−**15** was titrated with the corresponding complementary sequence (for example, see Figure 1), and the emission enhancement characteristics (ΔF) of the conjugated dyes were examined (Table 1). Both **12a** and **12b** exhibited ΔF values that were virtually identical, but only 60% of the value obtained for untethered **5** in the presence of the duplex dodecamer. The regioisomeric complexes **13a** and **13b** were similarly fluorescent, with **13a** exhibiting the more pronounced

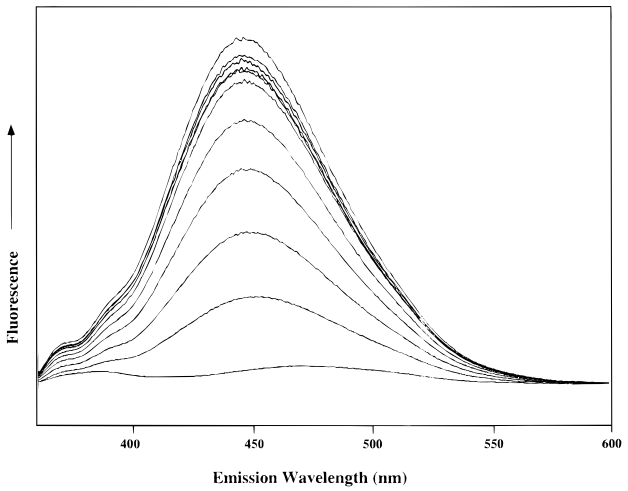

Figure 1. Fluorescence emission spectrum for a ~1 μM solution of **14a** titrated with aliquots of the complementary sequence 5′-d(CpGp-CpApApApApApApGpCpG).

effects, but the 7-fold enhancement must still be considered only a moderate effect. By comparison, **14a** with a nine-carbon linker resulted in a 23-fold enhancement in quantum yield (Figure 1, Table 1), slightly greater than the effect observed for untethered **9** in the presence of the dodecamer, and similar to the value observed for the untethered Hoechst 33258 (ΔF = 26). Emission characteristics for the complementary diastereomer **14b** were not as dramatic as those observed for **14a**, but this conjugate still exhibited a ΔF of 12, 65% of the value observed for untethered **9**. The regioisomeric conjugates **15a** and **15b** both exhibited significant ΔF values (12 and 11), but neither exhibited the dramatic enhancement observed for **14a**. A mixture of **14a**/**14b** (40:60) resulted in an intermediate value ($\Delta F \approx 15$).

To confirm that the observed fluorescence properties were the result of binding to the duplex DNA, we examined the temperature effects of the emission spectra. In all cases the fluorescence signal of the duplex conjugate was initially observed to decrease only marginally with temperature. But this initial effect was then followed by a more dramatic nonlinear decrease in quantum yield until a value was reached that was similar to that measured for the single-stranded conjugate. The transitions obtained for the various conjugated duplexes mirrored the transitions observed for a thermally induced helix-to-coil transition (Figure 2, and inset).

Discussion

The use of a site-specific thiol tether introduced to an internucleotide phosphate residue permits the postsynthetic conjugation of DNA sequences by a variety of agents. In the present work we have used fluorophores, analogues of the Hoechst minor-groove-binding bisbenzimidazoles, to prepare covalent DNA−Hoechst conjugates. These conjugates have been designed to permit normal hybridization between the conjugate DNA sequence and the target sequence. Hybridization by the conjugate to a target sequence converts a single-stranded species to a double-stranded complex and generates the B-form secondary structure with both the major and the minor grooves. In this respect, the hybridization event triggers a binding event by the tethered Hoechst fluorophore within the generated minor groove structure. The Hoechst fluorophores were chosen as a class of reagents for two reasons, the first being their affinity for the minor groove of duplex DNA containing dA-dT base pairs, and the second being the dramatic enhancement in emission maxima (>20-fold) observed with the

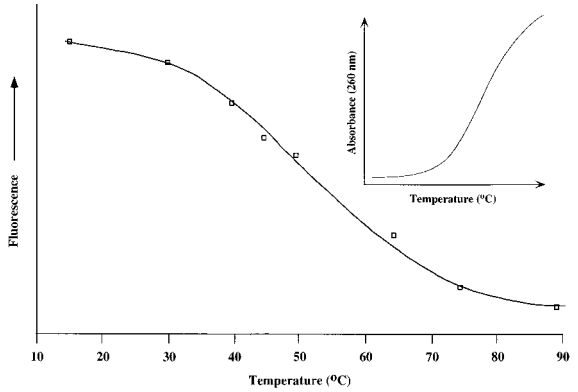

Figure 2. Fluorescence vs temperature plot for conjugate **14b** complexed to the complementary sequence 5′-d(CpGpCpTpTpTpTpTp-TpGpCpG). Inset: absorbance vs temperature plot for the same complex.

Hoechst dyes upon binding to double-stranded DNA sequences. The combination of a hybridization-triggered binding event, with the generation of a strong fluorescent signal, should provide the basis for the development of a DNA-based diagnostic, or *in situ* hybridization probe.

In the present work we have employed the internucleotide phosphate as the site for attachment of the groove-binding fluorophore in order to reduce any interference by the tethered fluorophore in the hybridization event. We note that conjugates such as **10**, carrying a large bulky substituent that is incapable of binding to the DNA sequence, can result in moderate reductions in the stability of the hybridization complex. However, conjugates **12**−**15** all resulted in increases (4−19 °C) in the T_m values for the hybridization complexes. A potential disadvantage in using the internucleotide phosphate as the tether site is that incorporation of the tether generates two diastereomers (R_p and S_p) about phosphorus. We had anticipated that this potential difficulty might be exploited in an advantageous manner if one of the two diastereomeric conjugates resulted in more effective helix stabilization or fluorescence characteristics. The four "**a**" diastereomers (Table 1) all result in nearly a 20 °C increase in their T_m values relative to that of the simple native duplex. The "**b**" diastereomers are also capable of enhancing the T_m values of the dodecamer duplexes, but only at more moderate levels (4−8 °C). This consistent increase in T_m values for the **a** diastereomers suggest that the positioning in the **a** diastereomers results in the fluorophore being more effectively oriented toward the minor groove (Figure 3) and, therefore, tentatively being assigned as the R_p diastereomers.[45] The **b** stereocenters are then the complementary S_p diastereomers. We note that the *pro-S* oxygens of the phosphodiester linkages (in both strands) are oriented toward the minor groove side of the phosphoribose backbone, while the *pro-R* oxygens are oriented toward the major groove side of the phosphoribose backbone. With respect to the position of the nitrogen in the corresponding phosphoramidate, these relative assignments are reversed[45] owing to atom priority in the stereocenter assignments.

In contrast to the differences in T_m values observed with the two diastereomeric conjugates, the positional differences had little effect upon the stability of the hybridization products.

(45) Owing to the vagaries of the Cahn−Ingold−Prelog system in assigning stereocenters, the S_p-phosphoramidate places the nitrogen of the P−N bond in the position occupied by the *pro-R*-oxygen of the internucleotide phosphodiester. Similarly, the absolute configurations of the S_p-phoshphoramidate and the R_p-phosphorothioates have the nitrogen and sulfur atoms in the same abolute positions. Correspondingly, the R_p-phosphoramidate then places the nitrogen into the position of the *pro-S*-oxygen of the internucleotide phosphate, and corresponds in configuration to the S_p-phosphorothioate.

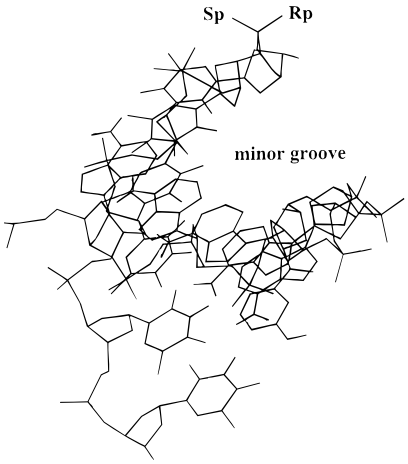

Figure 3. Duplex DNA containing the hexameric $(dA\text{-}dT)_6$ sequence with the relative sites that would be occupied by the nitrogens of a single phosphoramidate linkage marked as the R_p and S_p diastereomers. This graphic has been tilted so that the view is along the minor groove.

Regardless of whether the Hoechst derivative was oriented to follow the dT_5 residues (5′ → 3′) or was reversed, to follow the dA_5 residues (5′ → 3′), the resulting T_m values were virtually identical [compare **12a** (**12b**) with **13a** (**13b**), or **14a** (**14b**) with **15a** (**15b**)] (Table 1). These results suggest that the helix-stabilizing effects of the Hoechst derivatives are largely independent of the orientation of the fluorophore.

By comparison, the fluorescence emission spectra vary significantly among the various conjugated complexes. That the fluorescence effects result from binding to the duplex DNA structure can be inferred from the temperature studies performed. In all cases the fluorescence of the duplex conjugate decreased with increasing temperature, but these effects were most dramatic in the temperature range of the helix-to-coil transition (see Figure 2). This observation is consistent with the fluorophore being tightly bound within the minor groove where the excited state is largely protected from collisional decay processes involving bulk solvent, and in the bound state relaxes primarily through radiative decay.[15] As the complex undergoes a cooperative helix-to-coil transition, the excited state becomes more accessible to collisional processes, less relaxation by radiative decay occurs, and a more dramatic loss in quantum yield is observed. Owing to the cooperative nature of the helix-to-coil transition, a cooperative fluorescence vs temperature plot is obtained (Figure 2).

The relative enhancements in fluorescence emission spectra for the conjugates **12**−**15** vary depending upon the Hoechst derivative employed, and its orientation. For example, both diastereomers of conjugate **12**, as well as both diastereomers of **13**, exhibit significant (4-fold to 7-fold) enhancements in emission spectra, but these values are not nearly as dramatic as the roughly 26-fold enhancement observed for the parent, untethered Hoechst 33258, bound to the duplex dodecamer. Two explanations might account for the moderate fluorescence effects observed with these four diastereomeric conjugates. (i) The presence of the bromoacetamido linker alters the fluorescence characteristics of the dye/DNA complex. (ii) The length of the linker between the DNA backbone and the bisbenzimidazole will affect the positioning of the fluorophore within the groove structure. Consistent with the first explanation is the observation that 1 equiv of the Hoechst derivative **5** in the presence of duplex DNA resulted in only a moderate 9-fold enhancement in fluorescence. However, by adding to derivative **5** a short two-carbon linker (generating **9**), at least nominally to insulate the bromoacetamido linker from the bisbenzimidazole ring system, more dramatic fluorescence effects were observed. One equivalent of derivative **9** in the presence of duplex DNA now results in a 19-fold enhancement in fluorescence.

Lengthening the linker of the Hoechst derivative results overall in a longer tether between the dye and the DNA sequence. The addition of these two carbons increases the tether length to nine atoms and appears to permit optimal binding by the tethered fluorophore; both diastereomers of **14** and **15** (prepared from **9**) now exhibit at least an 11-fold increase in fluorescence when bound to their hybridization targets. The observation that the double-stranded complex formed from **14a** now exhibits the most dramatic effects, with a 23-fold enhancement in fluorescence, is also likely the result of an increased linker length. This difference in fluorescence effects for **14a** and **15a** suggests that one orientation of the bisbenzimidazole within the minor groove (that present in **14a**) is preferred with regard to attendant fluorescence effects. Orientation effects are difficult to correlate with the reported crystal structures[4] since self-complementary sequences are typically employed.

Conclusions

We have prepared two Hoechst 33258 analogues that permit their covalent attachment to DNA sequences. The hybridization of the DNA−Hoechst conjugates to target DNA generates the double-stranded hybridization product and thereby triggers the desired binding event in the minor groove by the tethered fluorophore. This binding event both enhances the stability of the hybridization complex and results in a fluorescent signal that reports on the success of the hybridization event. All of the tentatively assigned R_p diastereomeric conjugates result in DNA duplexes of similar stability, and in all cases they are more stable than the diastereomers tentatively assigned as the S_p stereocenters. The fluorescence properties of the complexes are more varied; one of the complexes exhibits a quantum yield enhancement that is very similar to that observed for the free untethered fluorophore. This observation suggests that the tether permits efficient binding by the fluorophore within the minor groove. The development of materials that are triggered by the hybridization event, to stabilize the hybridization product, and to signal the event with a dramatic increase in fluorescence, should provide the foundation for the development of a new class of DNA diagnostics or *in situ* hybridization probes.

Acknowledgment. This work was supported by a grant from the NIH (GM 37065). We thank Dr. Robert Kuimelis for critical reading of the paper.

Supporting Information Available: Figures showing the structure and UV/vis spectrum of **13**, HPLC analyses of the conjugate **12a** and dodecameric sequences, and the absorbance vs temperature plot for the duplex formed from conjugate **13a** and the complementary strand (5 pages). See any current masthead page for ordering and Internet access instructions.

JA960948M